



Journal of Geophysical Research: Solid Earth

Supporting Information for

Space-time monitoring of seafloor velocity changes using seismic ambient noise

Peng Guo^{1,2*}, Erdinc Saygin^{1,2} and Brian Kennett³

1. Deep Earth Imaging Future Science Platform, The Commonwealth Scientific and Industrial Research Organisation (CSIRO), Kensington 6151, WA, Australia.
2. Energy, The Commonwealth Scientific and Industrial Research Organisation (CSIRO), Kensington 6151, WA, Australia.
3. Research School of Earth Sciences, The Australian National University, Canberra, Australian Capital Territory 2601, Australia

Corresponding author: Peng Guo (peng.guo@csiro.au)

Contents of this file

Figures S1 to S10

Please note that, figures related to the Gorgon OBN survey are from Line 3924, unless otherwise stated.

Gorgon OBN Seismic Survey (2015-2016)

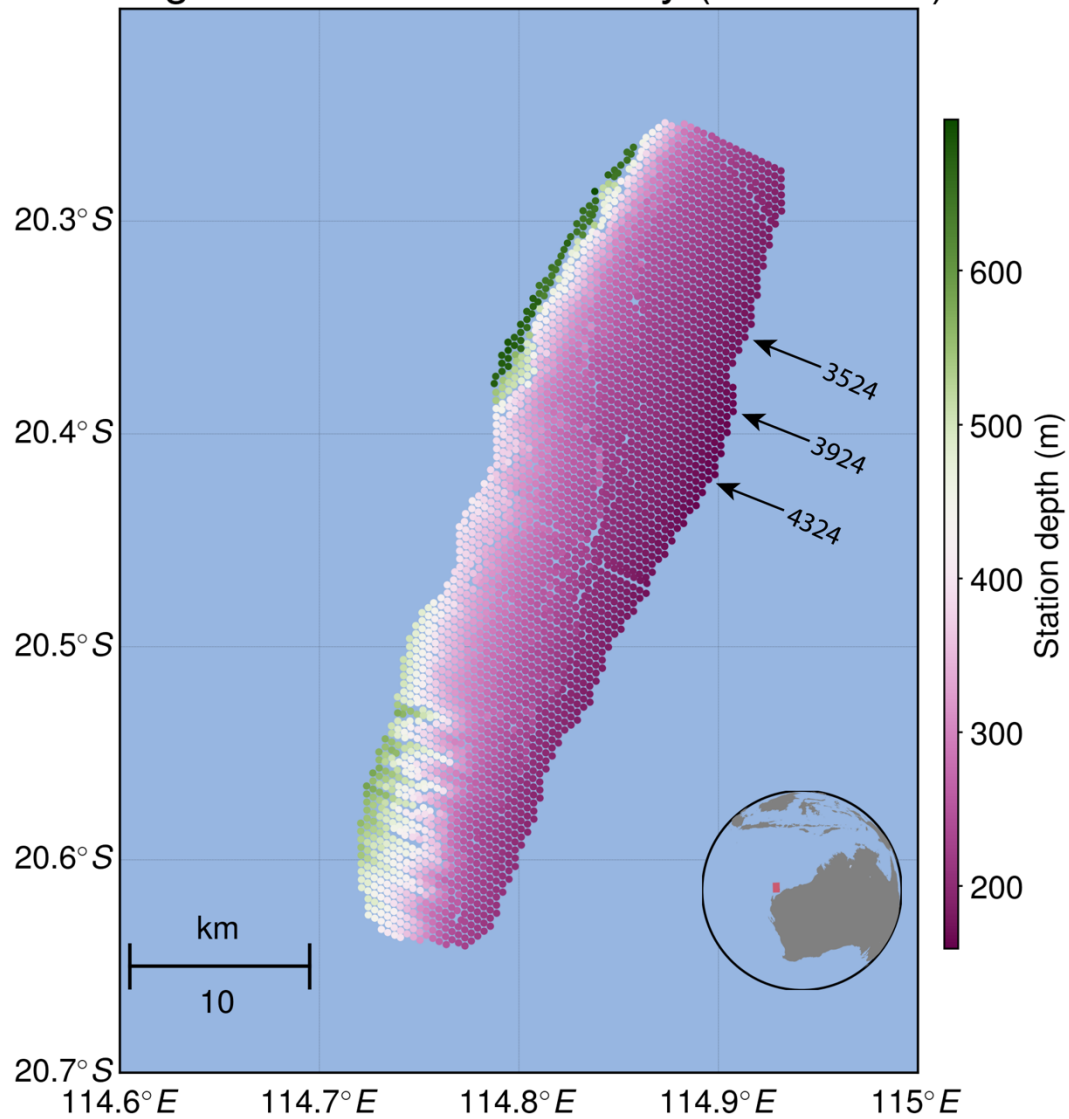


Figure S1. Ocean Bottom Node (OBN) seismic survey in the Gorgon gas field of the offshore of Western Australia by Chevron Australia and its partners. The colors on the OBNs suggest water depths. The black arrows indicate the positions of Line 3524, 3924 and 4324, respectively.

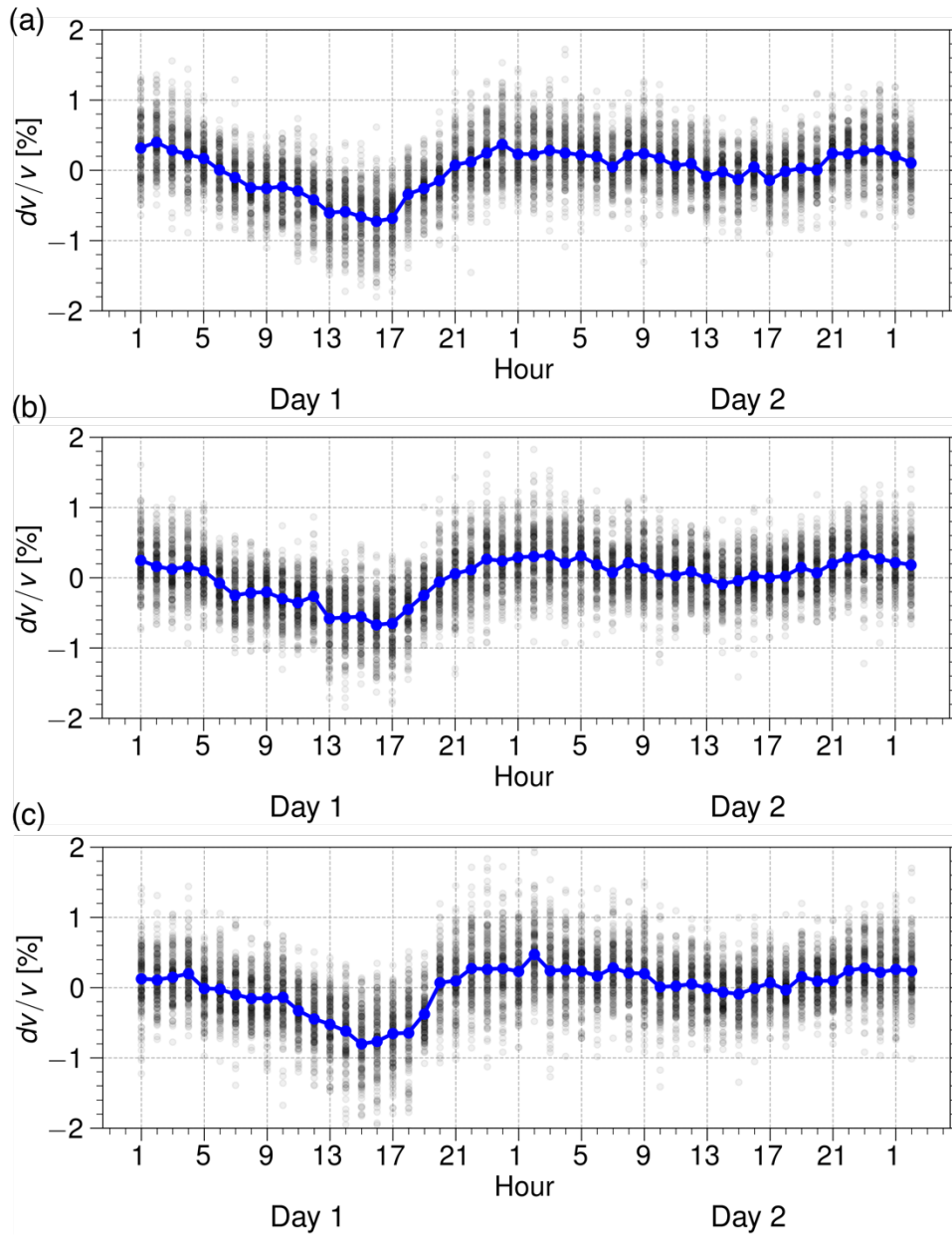


Figure S2. The shear-wave velocity changes (dv/v) of the seafloor on an hourly basis for Day 1 and Day 2 of 2016 from Lines (a) 3524, (b) 3924 and (c) 4324. The velocity changes were estimated using the ballistic part of the extracted Scholte waves of the CC functions.

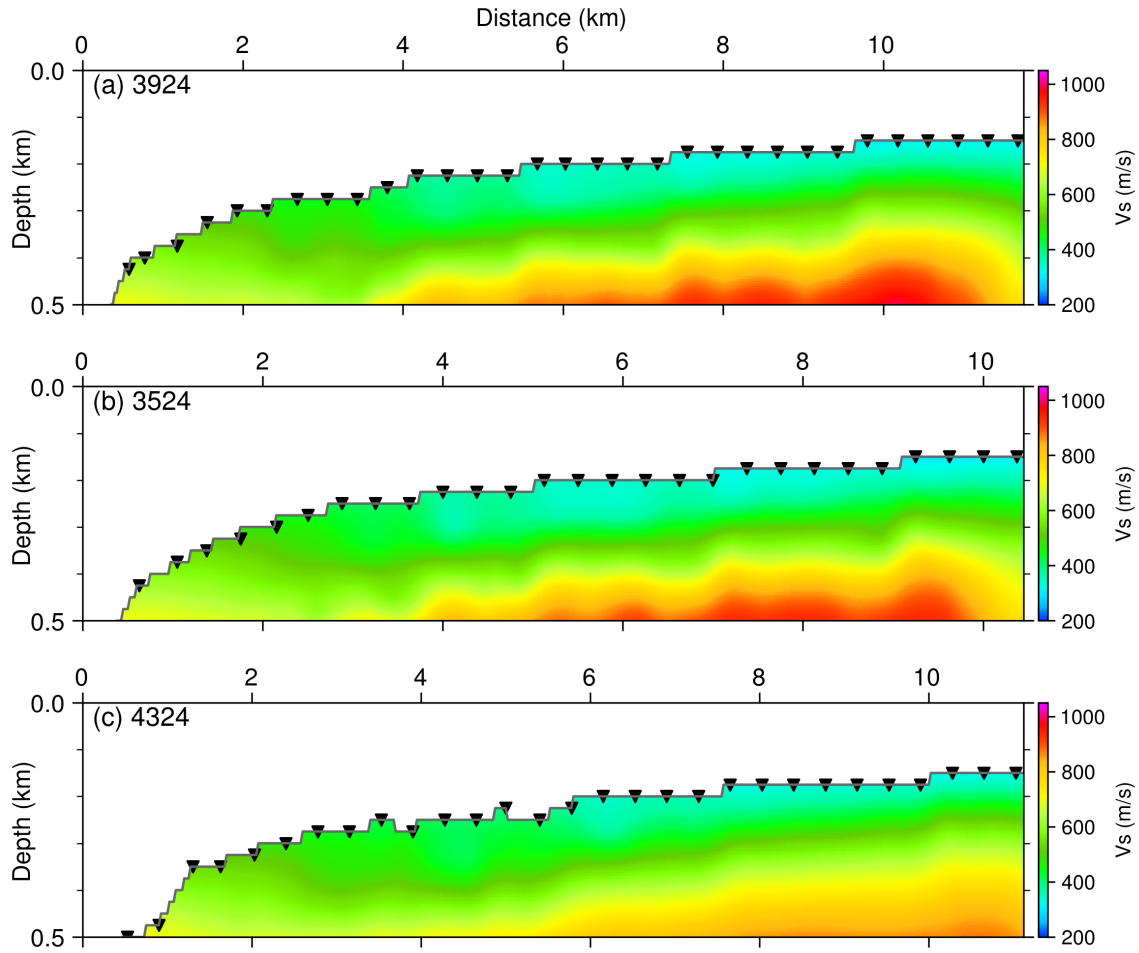


Figure S3. The velocity models from wave-equation dispersion inversion (Chen & Saygin, 2022), which are used as the starting models for reference (baseline) FWI. (a), (b) and (c) are the shear-wave velocity models for Line 3924, 3524 and 4324 (Figure S1), respectively.

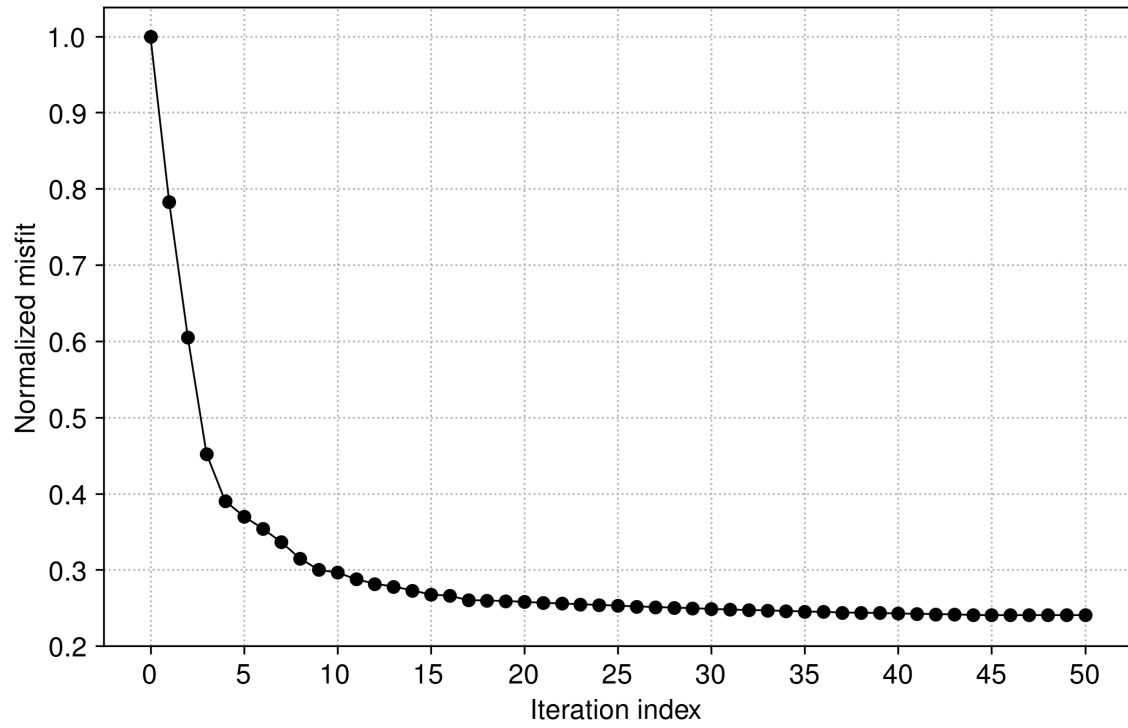


Figure S4. Waveform misfit as a function of iterations for trace-normalized FWI (baseline FWI). The waveform misfit was calculated using equation 1.

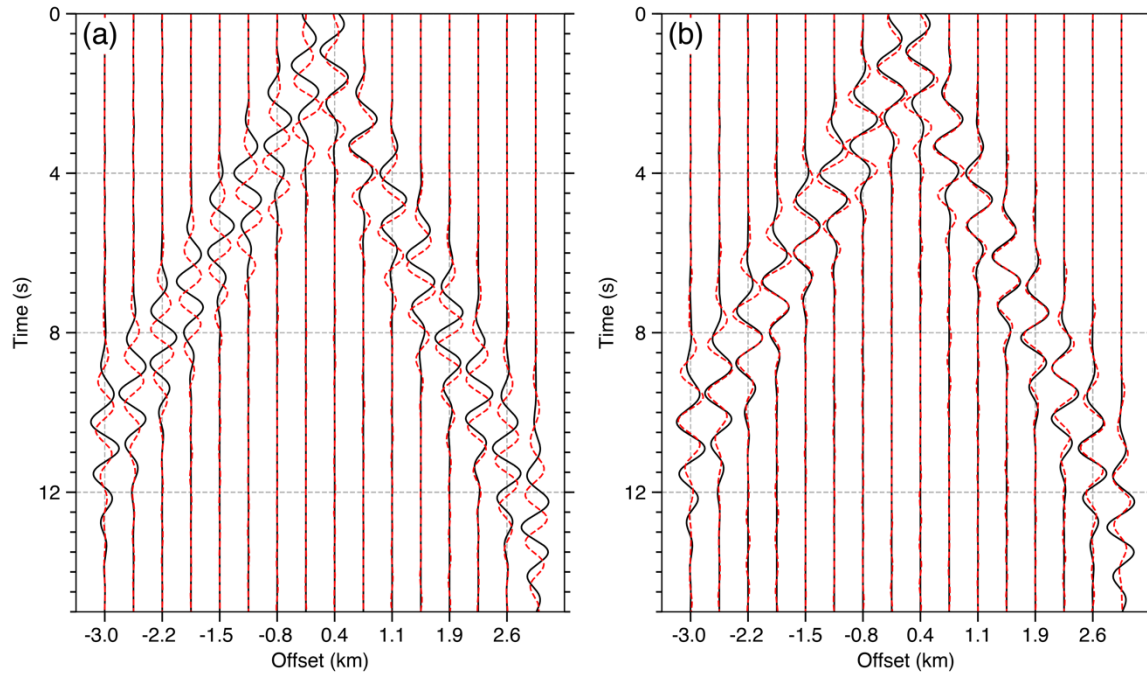


Figure S5. A comparison of observed (extracted from ambient noise) and synthetic seismic waveform data. (a) The observed data (black) and the synthetic waveform (dashed red) using the starting model (Fig. 6a) of reference FWI, and (b) the observed data (black) and the synthetic waveform (dashed red) using the final model from reference FWI (Fig. 6b). The waveform match between observed and synthetic data has been much improved after reference FWI.

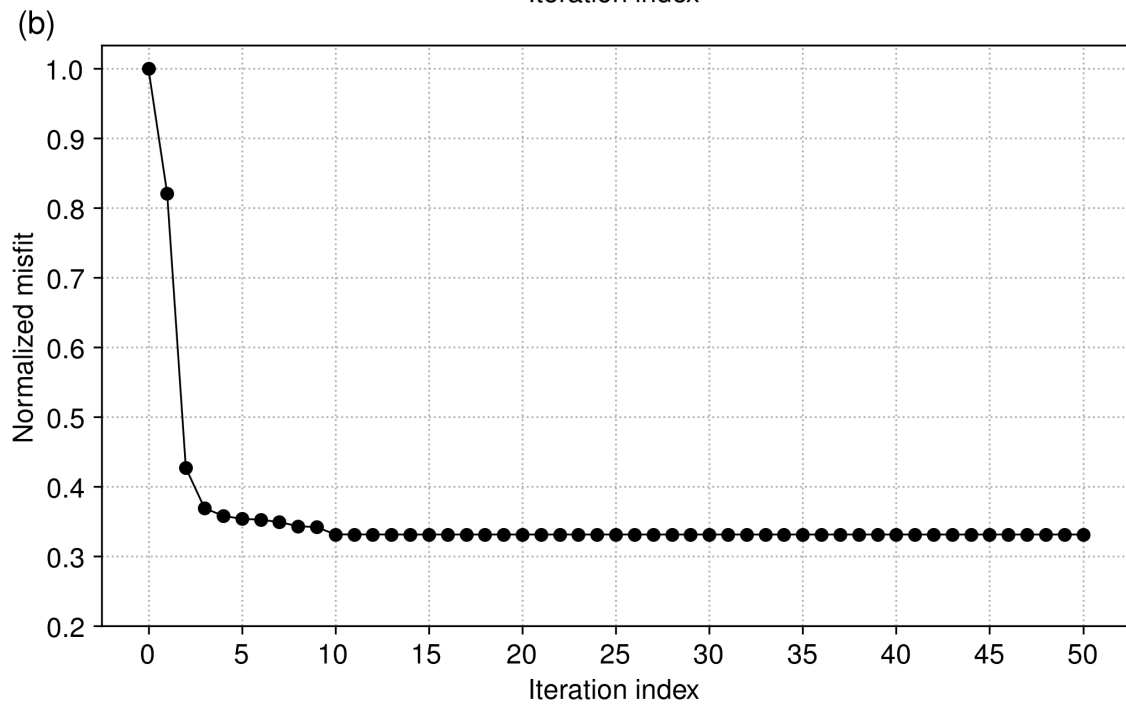
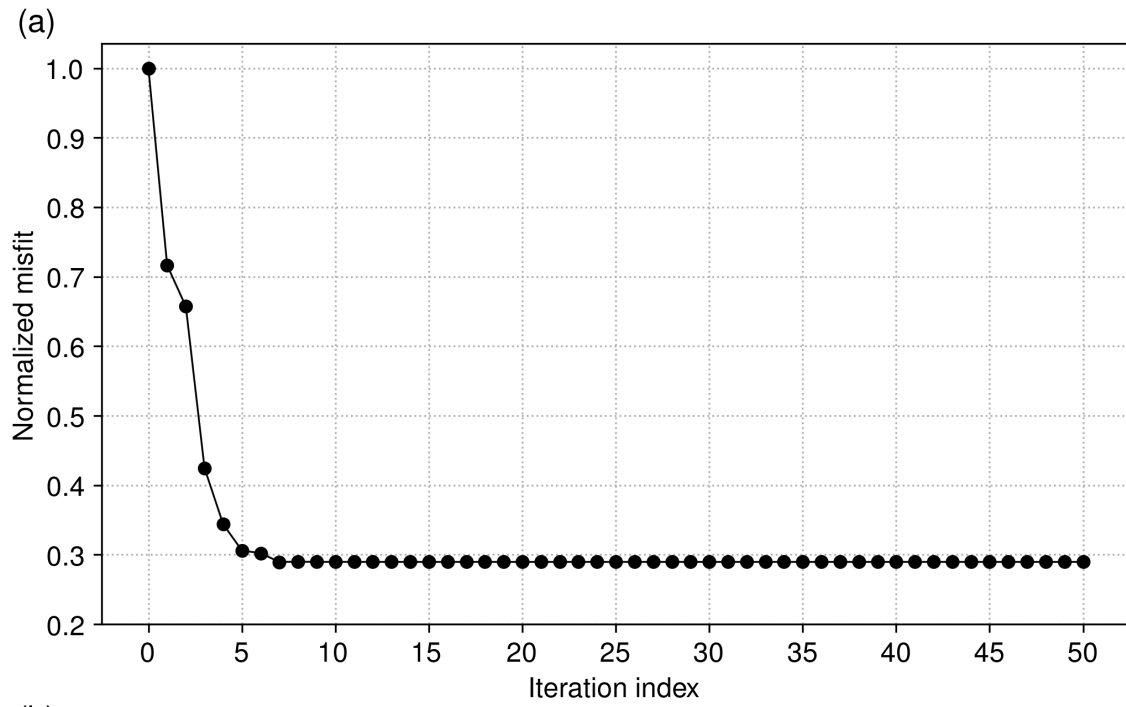


Figure S6. Misfit as a function of iterations for DD-WI, for (a) Hour 16 Day 1 and (b) Hour 2 Day 2. The misfit was calculated using equation 3.

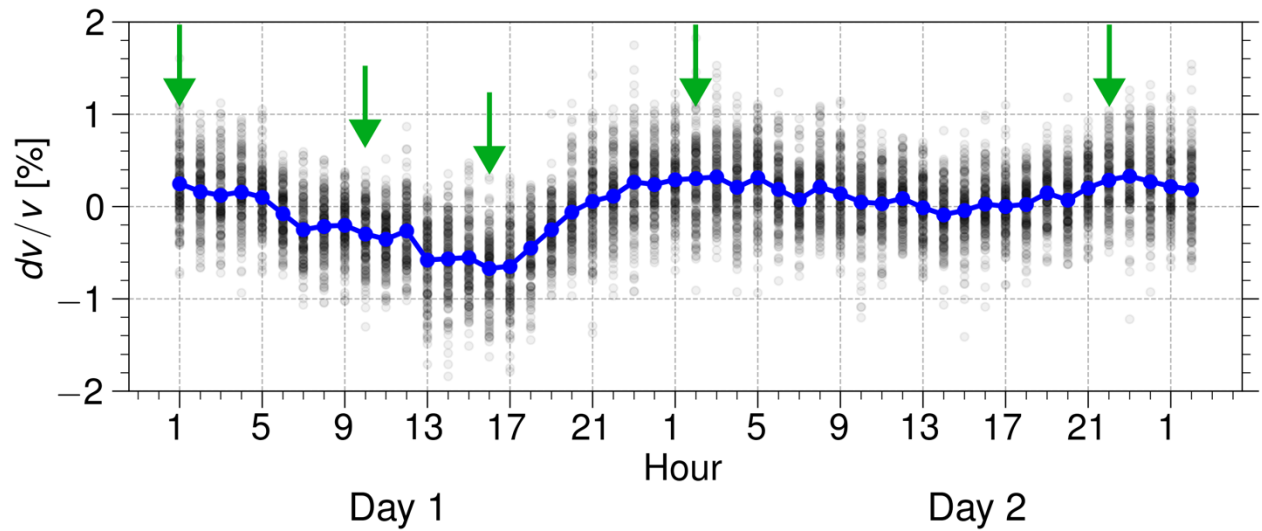


Figure S7. The relative shear-wave velocity changes (dv/v) of the seafloor on an hourly basis for Day 1 and Day 2 of 2016 (the same with Fig. 2a), assuming a spatially homogeneous dv/v . The green arrows from left to right indicate the dv/v for the time-lapse images in Figure 7 from top to bottom.

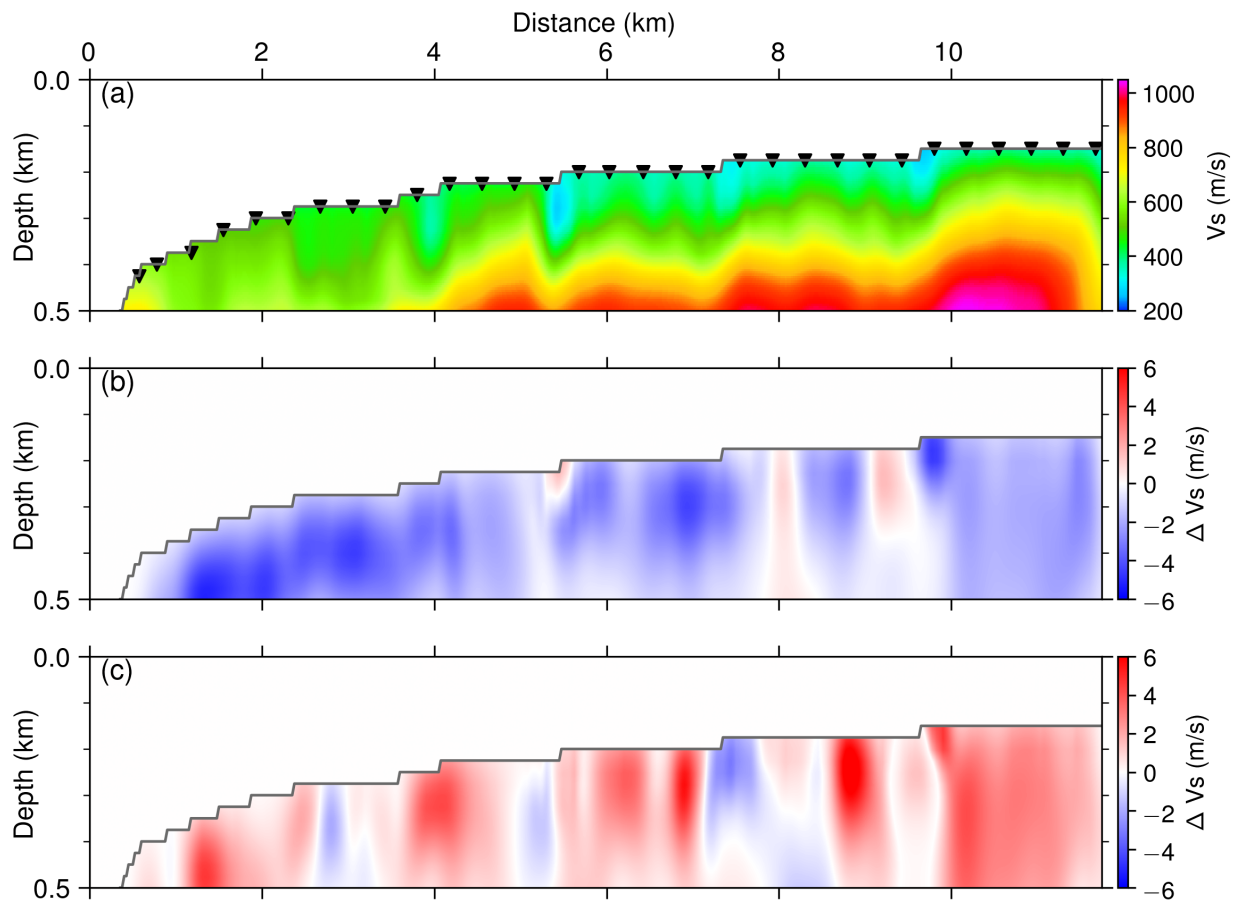


Figure S8. Reference velocity model and time-lapse subsurface models of velocity changes in the shallow seafloor for Line 3924. The starting model for baseline FWI is Fig. S3b. (a) The high-resolution baseline velocity model from trace-normalized FWI, which is used as the starting model for DD-WI. (b) The time-lapse image of velocity changes for Hour 15 Day 1. (c) The time-lapse image of velocity changes for Hour 1 Day 2. The black triangles in (a) indicate the locations of the OBNs.

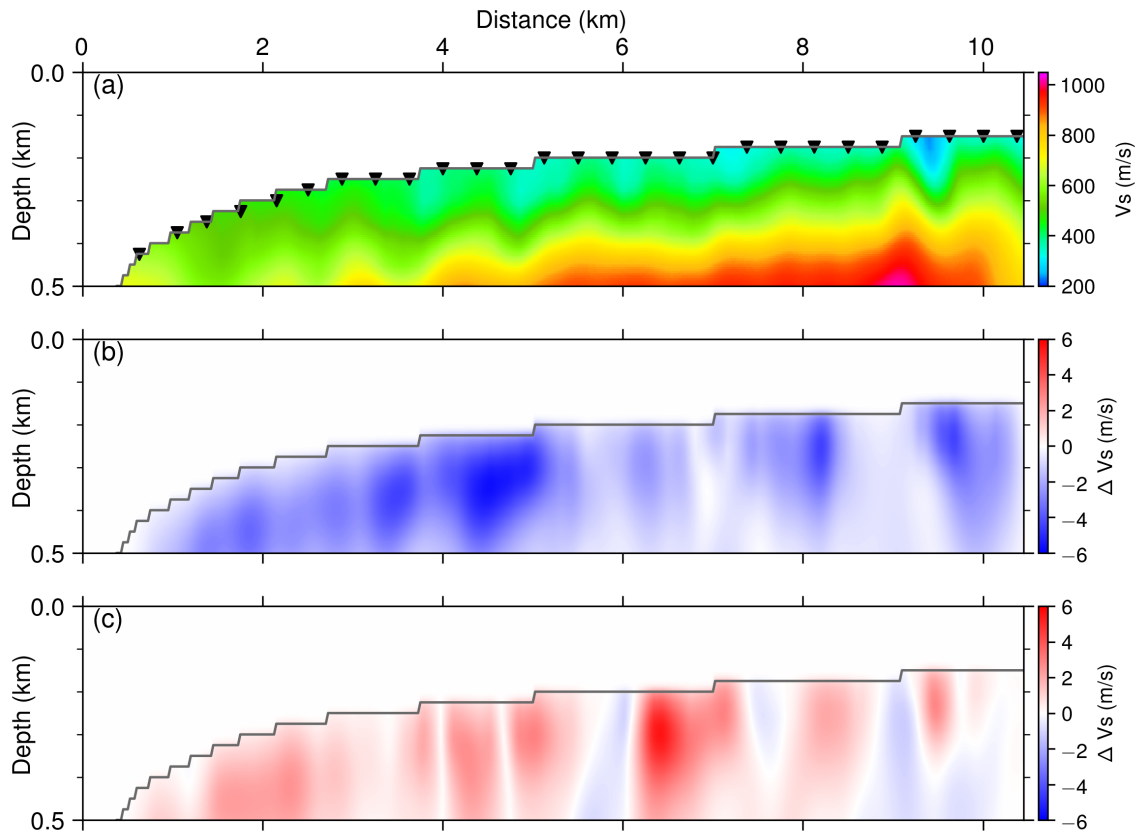


Figure S9. The same with Fig. S8 but for Line 4324 and the starting model for baseline FWI is Fig. S3b.

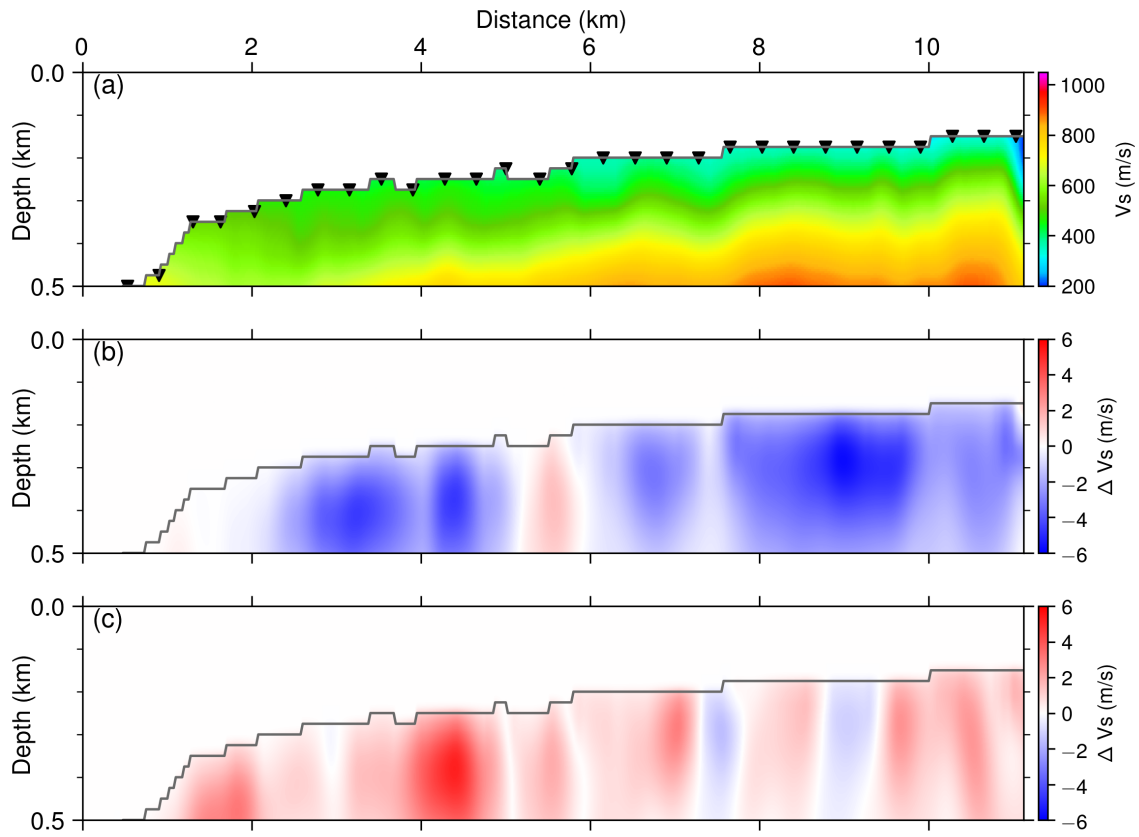


Figure S10. The same with Fig. S8 but for Line 4324 and the starting model for baseline FWI is Fig. S3c.